

## Accepted Manuscript

Title: Nucleotide coordination with 14 lanthanides studied by isothermal titration calorimetry

Authors: Zijie Zhang, Kiyoshi Morishita, Wei Ting David Lin, Po-Jung Jimmy Huang, Juewen Liu



PII: S1001-8417(17)30218-8  
DOI: <http://dx.doi.org/doi:10.1016/j.ccl.2017.06.014>  
Reference: CCLET 4108

To appear in: *Chinese Chemical Letters*

Received date: 4-4-2017  
Revised date: 21-4-2017  
Accepted date: 7-6-2017

Please cite this article as: Zijie Zhang, Kiyoshi Morishita, Wei Ting David Lin, Po-Jung Jimmy Huang, Juewen Liu, Nucleotide coordination with 14 lanthanides studied by isothermal titration calorimetry, Chinese Chemical Letters <http://dx.doi.org/10.1016/j.ccl.2017.06.014>

This is a PDF file of an unedited manuscript that has been accepted for publication. As a service to our customers we are providing this early version of the manuscript. The manuscript will undergo copyediting, typesetting, and review of the resulting proof before it is published in its final form. Please note that during the production process errors may be discovered which could affect the content, and all legal disclaimers that apply to the journal pertain.

Communication

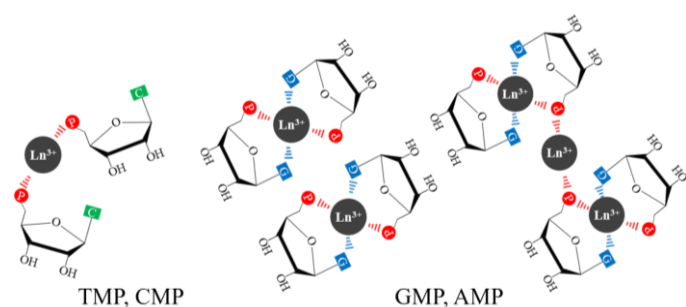
## Nucleotide coordination with 14 lanthanides studied by isothermal titration calorimetry

Zijie Zhang<sup>1</sup>, Kiyoshi Morishita<sup>1</sup>, Wei Ting David Lin, Po-Jung Jimmy Huang, Juewen Liu\**Department of Chemistry, Waterloo Institute for Nanotechnology, University of Waterloo, Waterloo N2L 3G1, Canada*

\* Corresponding author.

*E-mail address:* liujw@uwaterloo.ca<sup>1</sup> These authors contributed equally to this work.

## Graphical Abstract



ITC reveals the increasingly importance of entropy for heavier lanthanides binding to nucleotides. The phosphate group forming chelating effect with purine bases but not with pyrimidines.

## ARTICLE INFO

*Article history:*

Received

Received in revised form

Accepted

Available online

*Keywords:* DNA

Nucleic acids

Metal ions

Lanthanides

Entropy

## ABSTRACT

With their hydrolytic, optical and magnetic properties, lanthanide ions ( $\text{Ln}^{3+}$ ) are versatile probes for nucleic acids. In addition, nucleotide-coordinated  $\text{Ln}^{3+}$  ions form useful nanoparticles. However, the thermodynamic basis of their interaction is still lacking. In this work, isothermal titration calorimetry (ITC) is used to study the binding between nucleotides and 14 different  $\text{Ln}^{3+}$  ions.  $\text{Ln}^{3+}$  interacts mainly with the phosphate of cytidine and thymidine monophosphate (CMP and TMP), while the nucleobases in adenosine and guanosine monophosphate (AMP and GMP) are also involved. Phosphate binding is fully entropy driven since the reactions absorb heat. Nucleosides alone do not bind  $\text{Ln}^{3+}$  and the purines need the phosphate for chelation. With increasing atomic number of  $\text{Ln}^{3+}$ , the binding reaction with GMP goes from exothermic to endothermic. The entropy contribution starts to increase from  $\text{Gd}^{3+}$ , explaining the 'gadolinium break' observed in many  $\text{Ln}^{3+}$ -mediated RNA cleavage reactions. This study provides fundamental insights into the  $\text{Ln}^{3+}$ /nucleotide interactions, and it is useful for understanding related biosensors, nanomaterials, catalysts, and for lanthanide separation.

Lanthanides refer to a group of 15 elements from La to Lu. While they have been researched mostly for electronic, optical, and magnetic applications [1], lanthanide ions ( $\text{Ln}^{3+}$ ) are also useful tools in biochemistry. For example, nucleic acids enhance the luminescence of  $\text{Tb}^{3+}$  [2-4], which has been used for probing metal binding and designing biosensors [5].  $\text{Ln}^{3+}$  can cleave RNA at high metal concentrations [6,7]. Since cleavage activity is sensitive to RNA secondary structure, this is also useful for structural probing [8]. In addition,  $\text{Ln}^{3+}$  ions were used as metal cofactors in ribozymes and DNAzymes [3,9-17]. DNAzymes are DNA-based catalysts with promising applications in biosensor

development [18,19], gene silencing [20-23], nanotechnology [24], and bioinorganic chemistry and catalysis [25,26]. Finally, nucleotide-coordinated  $\text{Ln}^{3+}$  makes useful nanomaterials for enzyme encapsulation and sensing [27-32].

Based on their atomic number, lanthanides are divided into the light (La to Gd) and heavy (from Tb to Lu) groups, a useful distinction in describing their interaction with nucleic acids. A few studies have demonstrated the group trend of  $\text{Ln}^{3+}$  for interacting with nucleic acids. For example, the heavy lanthanides are much more active in cleaving a dinucleotide RNA junction [33]. Similar observations were also made in some RNA-cleaving DNAzymes: the GR5 [13], and Tm7 [16]; both are only active with the heavy lanthanides. Apparently, some properties change around  $\text{Gd}^{3+}$ , and this type of 'gadolinium break' has been often observed [13]. A few other nucleic acid enzymes (*e.g.* the Ce13d and leadzyme), however, have quite similar activities across the lanthanide series [12,14,15]. Finally, we recently used  $\text{Tb}^{3+}$  luminescence spectroscopy to study  $\text{Ln}^{3+}$  binding to DNA [34]. Most of these studies however, do not provide quantitative thermodynamic information.

Nucleic acids provide an interesting scaffold for lanthanide binding. They contain a negatively charged polyphosphate backbone that can strongly interact with lanthanides *via* electrostatic and Lewis acid/base interactions. At the same time, the four nucleobases with both oxygen and nitrogen based ligands may allow fine tuning of more specific coordination [35]. However, few previous works systematically studied their binding thermodynamics [36-41]. Isothermal titration calorimetry (ITC) is a powerful technique to study biomolecular binding, and a few studies reported on  $\text{Ln}^{3+}$  binding to nucleic acids [4,42]. Herein, we employ ITC to examine  $\text{Ln}^{3+}$  binding to nucleotides and nucleosides for the whole lanthanide series, revealing important thermodynamic trends and insights of their coordination.

We chose to use nucleoside monophosphates in this work to avoid complications related to folding and denaturation of nucleic acids by  $\text{Ln}^{3+}$ . In addition, we studied the basic structural units of nucleic acids: the nucleosides and phosphate. The molecules used in this study are shown in Fig. S1 (Supporting information). The ITC experiments were performed at pH 6 with 25 mmol/L NaCl. This condition is relevant to biochemical studies of  $\text{Ln}^{3+}$  interacting with nucleic acids. The light  $\text{Ln}^{3+}$  ions coordinate to nine water molecules, while the heavy ones are smaller and they coordinate to eight [43]. The change in coordination number occurs at  $\text{Gd}^{3+}$ . The first  $\text{pK}_a$  of  $\text{Ln}^{3+}$  ranges from 9.33 ( $\text{La}^{3+}$ ) to 8.17 ( $\text{Lu}^{3+}$ ) [44]. Therefore, at pH 6,  $\text{Ln}^{3+}$  remains largely as free non-hydrolyzed ions.

Since guanine is the most important nucleotide for sensitized  $\text{Ln}^{3+}$  luminescence [5,34], and for binding  $\text{Ln}^{3+}$  [45-47], we first studied guanosine monophosphate (GMP). By optimizing the experimental conditions, we found the background is lower by titrating lanthanides into nucleotides, instead of the other way (Fig. S2 in Supporting information). By integrating the heat, we obtained the binding curve, from which we can extract all the thermodynamic constants, including  $\Delta H$ ,  $\Delta S$ , the association constant ( $K$ ) and  $\Delta G$ .

After fixing the experimental conditions, a series of titrations were performed by injecting each respective  $\text{Ln}^{3+}$  into GMP (Fig. 1). Some interesting trends were observed. For example, binding of the light  $\text{Ln}^{3+}$  was accompanied with heat release, while the heavy ones resulted in heat absorption. The baselines are quite flat for each injection and the peaks are quite symmetric, indicating fast binding kinetics.

To have a complete understanding, we then repeated the experiment with other nucleotides. Instead of using all the 14  $\text{Ln}^{3+}$ , we chose  $\text{Nd}^{3+}$  and  $\text{Lu}^{3+}$  to represent light and heavy  $\text{Ln}^{3+}$ , respectively. When  $\text{Nd}^{3+}$  was titrated into AMP (Fig. 2A), the trace was quite similar to that of  $\text{Nd}^{3+}$  into GMP. Initially, the amount of heat released was large, and a typical binding curve was observed. The  $\Delta H$  of this reaction was calculated to be  $-1.97 \pm 0.15$  kcal/mol, which is slightly larger than that for  $\text{Nd}^{3+}$  into GMP ( $-1.40 \pm 0.29$  kcal/mol). When  $\text{Lu}^{3+}$  was titrated into AMP, the system showed a very small amount of heat response (Fig. 2F). However, we can at least conclude that the amount of heat released is much less (almost zero) compared to that of the  $\text{Nd}^{3+}$  titration. Interestingly, for TMP and CMP, the interactions were entropic, for both the light  $\text{Nd}^{3+}$  and the heavy  $\text{Lu}^{3+}$  (Figs. 2C, 2D, 2H, 2I). For both nucleotides, binding was much tighter to  $\text{Lu}^{3+}$  with more heat absorbed.

A nucleotide contains a phosphate and a nucleoside. To dissect the contribution of each component, we first probed the phosphate binding using ribose-5-phosphate (R5P, see Fig. S1B in Supporting information for structure), for which the base is removed. Phosphate is an important metal ligand in nucleic acids [48,49]. Its binding is endothermic (Figs. 2E and 2J), with the heavy  $\text{Ln}^{3+}$  absorbing much more heat (notice the different scale in the y-axis). This is quite similar to that of CMP and TMP. It is clear that purine and pyrimidine nucleotides have very different binding properties, and the pyrimidines rely on the phosphate for binding. For the purine nucleotides, binding also involves the bases.

After the phosphate, we then studied the nucleosides, and none of them gave much heat (Fig. S3 in Supporting information). This is not surprising since lanthanides are strong hard Lewis acids and the nucleosides are soft Lewis

bases. Therefore, without the phosphate, the interaction with the bases alone is weak, even for guanine. Taken together, the phosphate interaction is required for binding of  $\text{Ln}^{3+}$  to nucleotides. Without a base, the phosphate part can still bind, but not the other way around. However, the bases can influence phosphate binding, which explains the differences among the nucleotides. There might be some synergistic effects between the base and phosphate (*e.g.* chelating effect).

In the above results, we only described the data qualitatively. We then integrated the heat of each injection to obtain binding curves (Fig. 1 bottom panels), showing three types of possible coordination sites. An example illustrating these three sites is shown in Fig. S2F (Supporting information). For all the titrations, these three stages of binding were well separated. The affinity of stage 3 is drastically increased as the atomic number of  $\text{Ln}^{3+}$  increases. We calculated the thermodynamic parameters for all of the  $\text{Ln}^{3+}$  ions using a three-site model (Fig. 3, Table S1 in Supporting information).

The thermodynamic trends and values of site 1 (Figs. 3D, 3H, 3K) are very similar to those from site 2 (Figs. 3E, 3I, 3L). Therefore, we reason these two have the same chemical origin. The first site has a binding ratio of  $0.05 \pm 0.01$  for all the  $\text{Ln}^{3+}$  (Fig. 3A), meaning each  $\text{Ln}^{3+}$  can bind to 20 GMP molecules. This has far exceeded the chemically possible coordination number of  $\text{Ln}^{3+}$ . For comparison, site 2 has a ratio of  $0.5 \pm 0.04$  for all the  $\text{Ln}^{3+}$  (Fig. 3B). Therefore, site 1 is omitted from most of the subsequent discussion, due to its small binding ratio. It is likely that the binding of site 1 is due to the initial attraction of multiple GMP by each  $\text{Ln}^{3+}$  ion. As more  $\text{Ln}^{3+}$  was added, the initial complex broke to form the final binding complex. This process leads to an apparent two binding stages, but sites 1 and 2 likely have the same chemical origin. The second and third binding sites both have a  $\text{Ln}^{3+}$ -to-GMP ratio of  $0.5 \pm 0.06$  (Figs. 3B and 3C). After finishing all the binding reactions, the final ratio was still  $0.5 \pm 0.06$ , indicating that these binding reactions took place simultaneously and each  $\text{Ln}^{3+}$  could participate in both sites 2 and 3.

For each binding site, we obtained  $\Delta H$  and the association constant  $K$ . From  $K$ , the  $\Delta G$  was calculated and then  $\Delta S$  was calculated. For site 2, the enthalpy of binding goes from negative to positive and the point of transition is at  $\text{Dy}^{3+}$  (Fig. 3E). For the third binding site, the  $\Delta H$  is positive for all the  $\text{Ln}^{3+}$  (Fig. 3F). Therefore, binding at site 3 is fully entropy driven. For the second site, the binding affinity between  $\text{Ln}^{3+}$  and GMP is quite similar for all of the  $\text{Ln}^{3+}$  (Fig. 3I) at  $\sim 10^5$  L/mol ( $K_d = 10.2 \pm 3.5$   $\mu\text{mol/L}$ ). This binding affinity agrees with that from luminescence-based measurements [34]. Given the relatively small difference and the error bar size, we do not quantitatively describe the  $K_d$  trend here. Interestingly, for site 3, binding is very weak ( $K_d = 1.1 \pm 0.3$  mmol/L) for the first few light  $\text{Ln}^{3+}$ . Then, the binding affinity increased drastically reaching  $3.8 \pm 0.7$   $\mu\text{mol/L}$  for the last few heavy  $\text{Ln}^{3+}$  (Fig. 3J). The overall trend of entropy increased as the atomic number of  $\text{Ln}^{3+}$  increased for both sites 2 and 3 (Figs. 3L and 3M). Therefore, binding of the heavier  $\text{Ln}^{3+}$  is more entropy driven. It is interesting to note that the  $\Delta S$  difference between  $\text{Lu}^{3+}$  and  $\text{La}^{3+}$  is much larger for the third binding site than the second one.

We then examined the trend of entropy change (Figs. 3K-M). By considering only the metal ion and GMP, a binding reaction should decrease the entropy. The fact that entropy is increased for each  $\text{Ln}^{3+}$  binding to GMP is attributed to the associated water molecules.  $\text{Ln}^{3+}$  ions are highly hydrated and the number of associated water molecules changes from 9 for the lighter  $\text{Ln}^{3+}$  ions to 8 for the heavier ones. The change of water coordination number is attributed to the size contraction. For entropy related contributions, it is likely that the bound waters are released from the  $\text{Ln}^{3+}$  and inner-sphere interactions are achieved with GMP. For the lighter  $\text{Ln}^{3+}$ , the number of released water molecules may be smaller or the interaction might be more of an outer-sphere nature, with more bound water molecules remaining associated with these lanthanides after binding to GMP.

The standard entropy of liquid water is 16.7 cal/mol K. The entropy of water bound to metal salts is around 10 cal/mol K, regardless of the metal species [50]. Therefore, the entropy gain from releasing a bound water molecule is  $\sim 6.7$  cal/mol K. The entropy change of our system at its largest was  $32.7 \pm 1.5$  cal/mol K (Fig. 3M), which corresponded to the release of 5 water molecules. For the smaller  $\text{Ln}^{3+}$ , the number of released water molecules was 2-3. Therefore, the difference appears to be that more water molecules are released from the heavier  $\text{Ln}^{3+}$ . In every case, the  $\text{Ln}^{3+}$  ions were not completely dehydrated after binding. We ignored the release of water from GMP and the change of entropy due to GMP- $\text{Ln}^{3+}$  binding, but this description did provide a better physical picture of the difference between the light and heavy  $\text{Ln}^{3+}$ .

A question is why the larger  $\text{Ln}^{3+}$  ions tend to absorb heat. The enthalpy of hydration for  $\text{Ln}^{3+}$  becomes gradually more negative as the atomic number increases. For example,  $\text{Lu}^{3+}$  has the largest value of  $-898.3$  kcal/mol, compared to the value of  $-784.6$  kcal/mol for  $\text{La}^{3+}$  [44]. In addition, the number of coordinated water molecules decreases from 9 to 8 from  $\text{La}^{3+}$  to  $\text{Lu}^{3+}$ . Therefore, the energy cost of dehydration is nearly 30% more for  $\text{Lu}^{3+}$  than that for  $\text{La}^{3+}$ .

(112.3 kcal/mol for  $\text{Lu}^{3+}$  vs. 87.1 kcal/mol for  $\text{La}^{3+}$ ), which can explain the heat absorption required for binding heavier  $\text{Ln}^{3+}$ .

None of the nucleosides produced much heat with  $\text{Ln}^{3+}$  (Fig. S3 in Supporting information), indicating very weak interaction with the bases and the sugar ring. When a phosphate and nucleosides are linked to form nucleotides, new interactions can take place due to the chelation effect. Based on the heat profile from ITC titrations, TMP and CMP behave like R5P. In other words, their phosphate interaction dominates (true for both light and heavy  $\text{Ln}^{3+}$ ). We also quantitatively fitted the four nucleotides plus R5P (Fig. 4, Table S2 in Supporting information). The three site-model was applied also to AMP. We did not show site 1 since it again had a very low ratio of  $<0.05$ . For CMP, TMP and R5P, we only used a two-site model (site 1 and 3) since site 2 could not be identified in their binding curves. For these three, the contribution of site 1 was also less than 0.05 and thus we also omitted them for discussion.  $\text{Ln}^{3+}$  binding to AMP and GMP is more influenced by the bases. For example, when the light  $\text{Ln}^{3+}$  interacted with AMP or GMP, there was an overall release of heat in the initial ITC profile.

By observing the ITC profiles of R5P, the enthalpy term is unfavorable for either light or heavy  $\text{Ln}^{3+}$ . Therefore, its binding of  $\text{Ln}^{3+}$  is fully entropy driven. As such,  $\text{Ln}^{3+}$  ions interact with the phosphate *via* inner-sphere coordination and the coordinated water molecules are lost (thus inner sphere). This is reasonable since phosphate is a strong ligand for  $\text{Ln}^{3+}$ . The interaction between  $\text{Ln}^{3+}$  and the purine base of GMP or AMP is likely outer-sphere coordination. This interaction resulted in a reduction in enthalpy (negative  $\Delta H$ ). A difference between light and heavy  $\text{Ln}^{3+}$  is that for light  $\text{Ln}^{3+}$ , the enthalpy contribution from the purine interaction is enough to overcome the effects of the phosphate interaction and the net result is a release of heat. For heavy  $\text{Ln}^{3+}$ , the heat release of the purine interaction is insufficient to overcome the larger heat absorbed in the phosphate interaction and the result is an overall enthalpically unfavourable process.

*Via* extensive spectroscopic studies [51-53], it was concluded that in acidic pH,  $\text{Ln}^{3+}$  undergoes inner-sphere coordination with the phosphate, and outer-sphere coordination with the N7 of guanine. We reason that the chemical origin of the second binding site is the chelation of  $\text{Ln}^{3+}$  by the phosphate and the guanine base, which might take place at the O6 and N7 positions [46,48,54]. Given the similarity of the ITC profiles between AMP and GMP and previous literature, we tend to believe that the N7 site is more important, which is common in these two nucleotides.

ITC also gives insight into the binding stoichiometry. For all of the lanthanides, a final binding ratio of  $0.5 \pm 0.06$  is observed, meaning that every lanthanide ion binds to two GMP molecules, regardless of the size of the lanthanide. For GMP and AMP, binding site 2 originated from the chelation of phosphate and the purine base, and binding site 3 was purely from the remaining coordination power of the phosphate. Since the  $K_d$  of these two sites are similar for the heavy lanthanides, binding to these two sites are taking place simultaneously (Fig. 5B). For the light lanthanides, site 2 might be filled first since it has much higher affinity than site 3 (Fig. 5A). For CMP, TMP and R5P, the main interactions are with the phosphate part and this explains that we mainly see one type of site in Fig. 3 for them (site 3) (Fig. 5C). Note that these binding configurations are hypothesized based on our ITC data, and further confirmation requires more rigorous structural biology tools such as NMR and X-ray crystallography.

Our interest on the lanthanides is from *in vitro* selection of RNA-cleaving DNAzymes using  $\text{Ln}^{3+}$  as a cofactor [14-16,55-57]. Most of the DNAzymes showed a clear lanthanide size-dependent activity trend [55]. In every case, binding of  $\text{Ln}^{3+}$  to the scissile phosphate is critical since it can neutralize the negative charge in the transition state. So far, we have observed a few types of behavior in lanthanide trends for DNAzyme catalysis. For the Lu12 and Ce5 DNAzymes, their activity gradually decreased as the atomic number of  $\text{Ln}^{3+}$  increased [14,57]. This continuous trend agrees well with the thermodynamic trends reported here for the GMP interactions. Note that the scissile phosphate in our system is flanked immediately by a guanine and an adenine, both are purine nucleotides. The Ce13d DNAzyme binds only one  $\text{Ln}^{3+}$  ion and it has a very similar activity with all the other lanthanides [15,58]. This may suggest an outer-sphere interaction to some extent such that the charge of the metal is more important.

In summary, we performed systematic ITC experiments to study the interaction between four types of nucleotides and 14 lanthanide ions. Purine nucleotides interact with  $\text{Ln}^{3+}$  *via* both the phosphate and nucleobase, and there is a synergistic chelation effect between these two groups. Pyrimidine nucleotides interact with  $\text{Ln}^{3+}$  mainly *via* the phosphate group, with little contribution from the bases. With increasing atomic number of  $\text{Ln}^{3+}$ , the interactions with phosphate increase, explaining the better efficiency of heavy  $\text{Ln}^{3+}$  as a cofactor for some DNAzymes. From quantitative thermodynamic calculations, lanthanide binding is mainly driven by entropy from released water molecules during the binding reaction, especially for the heavy lanthanides. The release of water suggests inner sphere coordination, thus making it easier to distinguish heavy lanthanides than light ones. The thermodynamic

insights from this study can be used to explain the lack of nanoparticle formation with TMP, CMP, and  $\text{Ln}^{3+}$ . In addition, it rationalizes the simple and more complex trend of  $\text{Ln}^{3+}$  activity in various DNAzymes by changing the number of ions involved. Such insights are useful for guiding rational ligand design for better separation of these important metals.

## Acknowledgment

Funding for this work is from the Natural Sciences and Engineering Research Council of Canada (NSERC).

## References

- [1] D. Parker, R. S. Dickins, H. Puschmann, C. Crossland, J. A. K. Howard, *Chem. Rev.* 102 (2002) 1977-2010.
- [2] A. L. Feig, M. Panek, W. D. Horrocks Jr, O. C. Uhlenbeck, *Chem. Biol.* 6 (1999) 801-810.
- [3] H.-K. Kim, J. Li, N. Nagraj, Y. Lu, *Chem. Eur. J.* 14 (2008) 8696-8703.
- [4] C. Mundoma, N. L. Greenbaum, *J. Am. Chem. Soc.* 124 (2002) 3525-3532.
- [5] M. Zhang, H.-N. Le, X.-Q. Jiang, B.-C. Yin, B.-C. Ye, *Anal. Chem.* 85 (2013) 11665-11674.
- [6] M. Komiyama, N. Takeda, H. Shigekawa, *Chem. Commun.* (1999) 1443-1451.
- [7] S. J. Franklin, *Curr. Opin. Chem. Biol.* 5 (2001) 201-208.
- [8] N. G. Walter, N. Yang, J. M. Burke, *J. Mol. Biol.* 298 (2000) 539-555.
- [9] A. L. Feig, W. G. Scott, O. C. Uhlenbeck, *Science* 279 (1998) 81-84.
- [10] V. Dokukin, S. K. Silverman, *Chem. Sci.* 3 (2012) 1707-1714.
- [11] F. Javadi-Zarnaghi, C. Hobartner, *J. Am. Chem. Soc.* 135 (2013) 12839-12848.
- [12] N. Sugimoto, T. Ohmichi, *FEBS Lett.* 393 (1996) 97-100.
- [13] C. R. Geyer, D. Sen, *J. Mol. Biol.* 275 (1998) 483-489.
- [14] P.-J. J. Huang, M. Vazin, J. Liu, *Anal. Chem.* 86 (2014) 9993-9999.
- [15] P.-J. J. Huang, J. Lin, J. Cao, M. Vazin, J. Liu, *Anal. Chem.* 86 (2014) 1816-1821.
- [16] P.-J. J. Huang, M. Vazin, Z. Matuszek, J. Liu, *Nucleic Acids Res.* 43 (2015) 461-469.
- [17] W. Zhou, J. Ding, J. Liu, *ChemBioChem* 17 (2016) 1563-1570.
- [18] J. Liu, Z. Cao, Y. Lu, *Chem. Rev.* 109 (2009) 1948-1998.
- [19] Y. S. Huang, X. M. Wu, T. Tian, et al., *Sci. China Chem.* 60 (2017) 293-298.
- [20] G. F. Joyce, *Ann. Rev. Biochem.* 73 (2004) 791-836.
- [21] K. Schlosser, Y. F. Li, *Chem. Biol.* 16 (2009) 311-322.
- [22] W. H. Zhou, J. S. Ding, J. W. Liu, *Theranostics* 7 (2017) 1010-1025.
- [23] F. Huanhuan, Z. Xiaobing, L. Yi, *Sci. China Chem.* 60 (2017) 591-601.
- [24] L. H. Tan, H. Xing, Y. Lu, *Acc. Chem. Res.* 47 (2014) 1881-1890.
- [25] K. Hwang, P. Hosseinzadeh, Y. Lu, *Inorg. Chim. Acta* 452 (2016) 12-24.
- [26] S. K. Silverman, *Trends Biochem. Sci.* 41 (2016) 595-609.
- [27] R. Nishiyabu, N. Hashimoto, T. Cho, et al., *J. Am. Chem. Soc.* 131 (2009) 2151-2158.
- [28] Y. Liu, Z. Tang, *Chem. Eur. J.* 18 (2012) 1030-1037.
- [29] F. Wang, B. Liu, P.-J. J. Huang, J. Liu, *Anal. Chem.* 85 (2013) 12144-12151.
- [30] Q. Yuan, Y. Wu, J. Wang, et al., *Angew. Chem. Int. Ed.* 52 (2013) 13965-13969.
- [31] J. Wang, T. Wei, X. Li, et al., *Angew. Chem. Int. Ed.* 53 (2014) 1616-1620.
- [32] F. Wang, Y. Han, C. S. Lim, et al., *Nature* 463 (2010) 1061-1065.
- [33] K. Matsumura, M. Komiyama, *J. Biochem.* 122 (1997) 387-394.
- [34] W. T. D. Lin, P.-J. J. Huang, R. Pautler, J. Liu, *Chem. Commun.* 50 (2014) 11859-11862.
- [35] Z. Kolarik, *Chem. Rev.* 108 (2008) 4208-4252.
- [36] R. M. Izatt, J. J. Christensen, J. H. Rytting, *Chem. Rev.* 71 (1971) 439-482.
- [37] M. S. Singh, N. Homendra, R. K. Lonibala, *Biometals* 25 (2012) 1235-1246.
- [38] H. A. Azab, Z. M. Anwar, R. G. Ahmed, *J. Chem. Eng. Data* 55 (2010) 459-475.
- [39] A. S. Orabi, H. A. Azab, F. Saad, H. Said, *J. Sol. Chem.* 39 (2010) 319-334.
- [40] H. A. Azab, S. S. Al-Deyab, Z. M. Anwar, I. I. Abd El-Gawad, R. M. Kamel, *J. Chem. Eng. Data* 56 (2011) 2613-2625.
- [41] R. M. Smith, A. E. Martell, Y. Chen, *Pure Appl. Chem.* 63 (1991) 1015-1080.
- [42] N. L. Greenbaum, C. Mundoma, D. R. Peterman, *Biochemistry* 40 (2001) 1124-1134.
- [43] D. G. Karraker, *J. Chem. Edu.* 47 (1970) 424.
- [44] J. Burgess, *Metal Ions in Solution*, 1st. ed., Ellis Horwood Ltd., Chichester, 1978.
- [45] G. Yonuschot, D. Helman, G. Mushrush, G. Vandewoude, G. Robey, *Bioinorg. Chem.* 8 (1978) 405-418.
- [46] P. K. L. Fu, C. Turro, *J. Am. Chem. Soc.* 121 (1999) 1-7.

- [47]D. Ringer, S. Burchett, D. Kizer, *Biochemistry* 17 (1978) 4818-4824.
- [48]R. K. O. Sigel, H. Sigel, *Acc. Chem. Res.* 43 (2010) 974-984.
- [49]H. Sigel, R. Griesser, *Chem. Soc. Rev.* 34 (2005) 875.
- [50]J. D. Dunitz, *Science* 264 (1994) 670.
- [51]S. L. Klakamp, W. D. Horrocks, *Biopolymers* 30 (1990) 33-43.
- [52]H.-A. Tajmir-Riahi, *Biopolymers* 31 (1991) 1065-1075.
- [53]D. Gersanovski, P. Colson, C. Houssier, E. Fredericq, *Biochim. Biophys. Acta* 824 (1985) 313-323.
- [54]R. K. O. Sigel, *Angew. Chem. Int. Ed.* 46 (2007) 654-656.
- [55]P.-J. J. Huang, M. Vazin, J. J. Lin, R. Pautler, J. Liu, *ACS Sensors* 1 (2016) 732-738.
- [56]P.-J. J. Huang, M. Vazin, J. Liu, *Biochemistry* 55 (2016) 2518-2525.
- [57]W. Zhou, J. Ding, J. Liu, *ChemBioChem* 17 (2016) 890-894.
- [58]M. Vazin, P.-J. J. Huang, Ż. Matuszek, J. Liu, *Biochemistry* 54 (2015) 6132-6138.

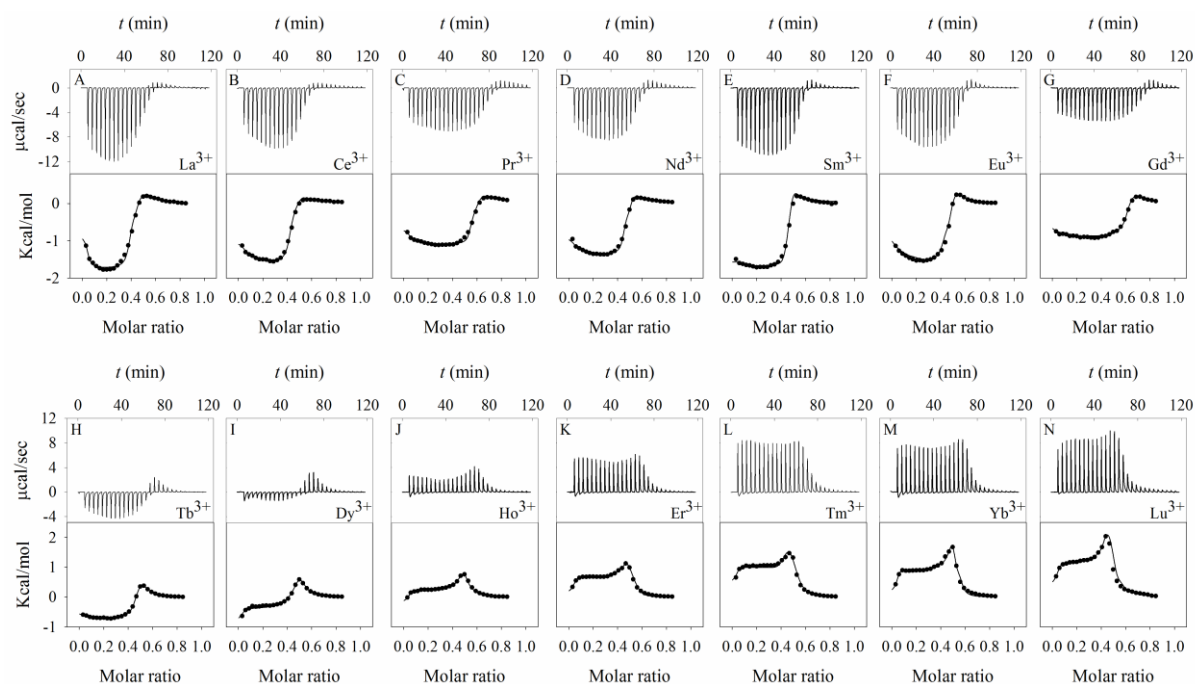


**Fig. 1.** The complete ITC titration traces of 14  $\text{Ln}^{3+}$  ions into GMP in the buffer A at 297 K: (A)  $\text{La}^{3+}$ ; (B)  $\text{Ce}^{3+}$ ; (C)  $\text{Pr}^{3+}$ ; (D)  $\text{Nd}^{3+}$ ; (E)  $\text{Sm}^{3+}$ ; (F)  $\text{Eu}^{3+}$ ; (G)  $\text{Gd}^{3+}$ ; (H)  $\text{Tb}^{3+}$ ; (I)  $\text{Dy}^{3+}$ ; (J)  $\text{Ho}^{3+}$ ; (K)  $\text{Er}^{3+}$ ; (L)  $\text{Tm}^{3+}$ ; (M)  $\text{Yb}^{3+}$  and (N)  $\text{Lu}^{3+}$ . Each peak corresponds to an injection of 200 nmol of  $\text{Ln}^{3+}$  into a fixed 7.275  $\mu\text{mol}$  of GMP. Background heat of titrating  $\text{Ln}^{3+}$  into buffer was subtracted. The integrated heat of each titration is also shown and the data points were fitted to extract thermodynamic parameters.



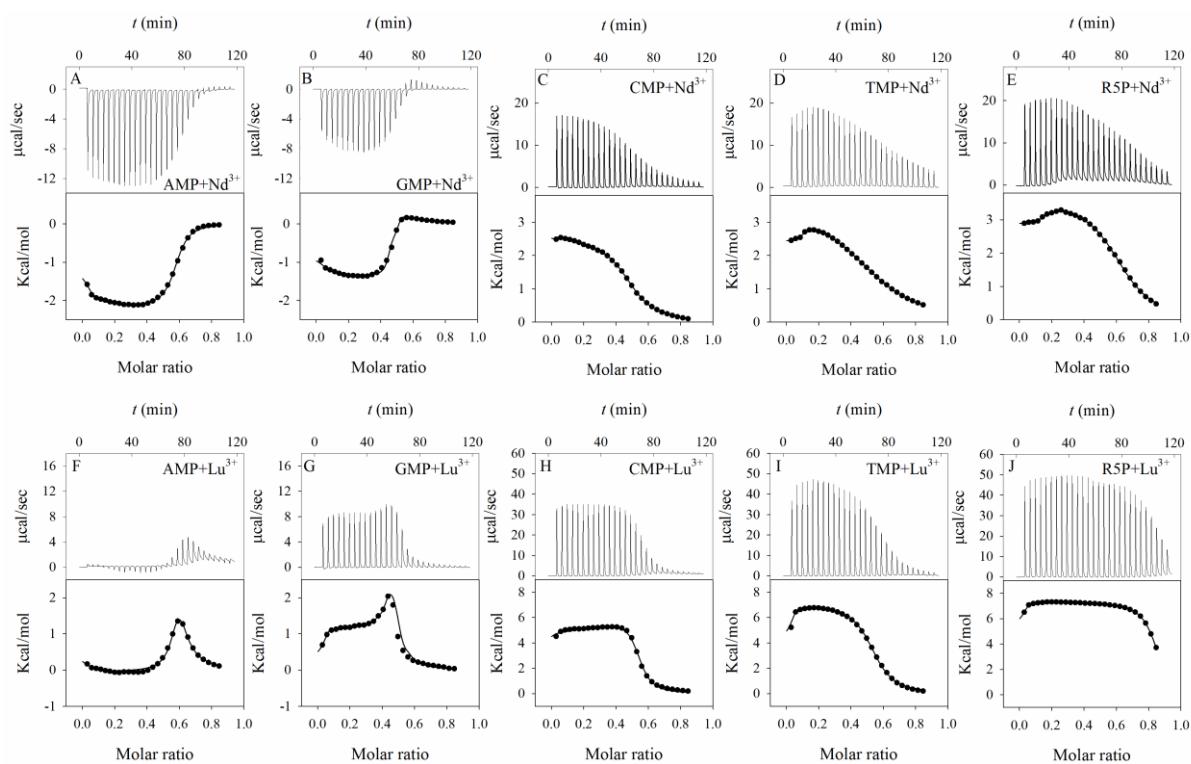


**Fig. 2.** ITC traces of  $\text{Nd}^{3+}$  into 5 mmol/L (A) AMP, (B) GMP, (C) CMP, (D) TMP and (E) ribose 5-phosphate (R5P). ITC traces of  $\text{Lu}^{3+}$  into 5 mmol/L (F) AMP, (G) GMP, (H) CMP, (I) TMP and (J) ribose 5-phosphate (R5P).

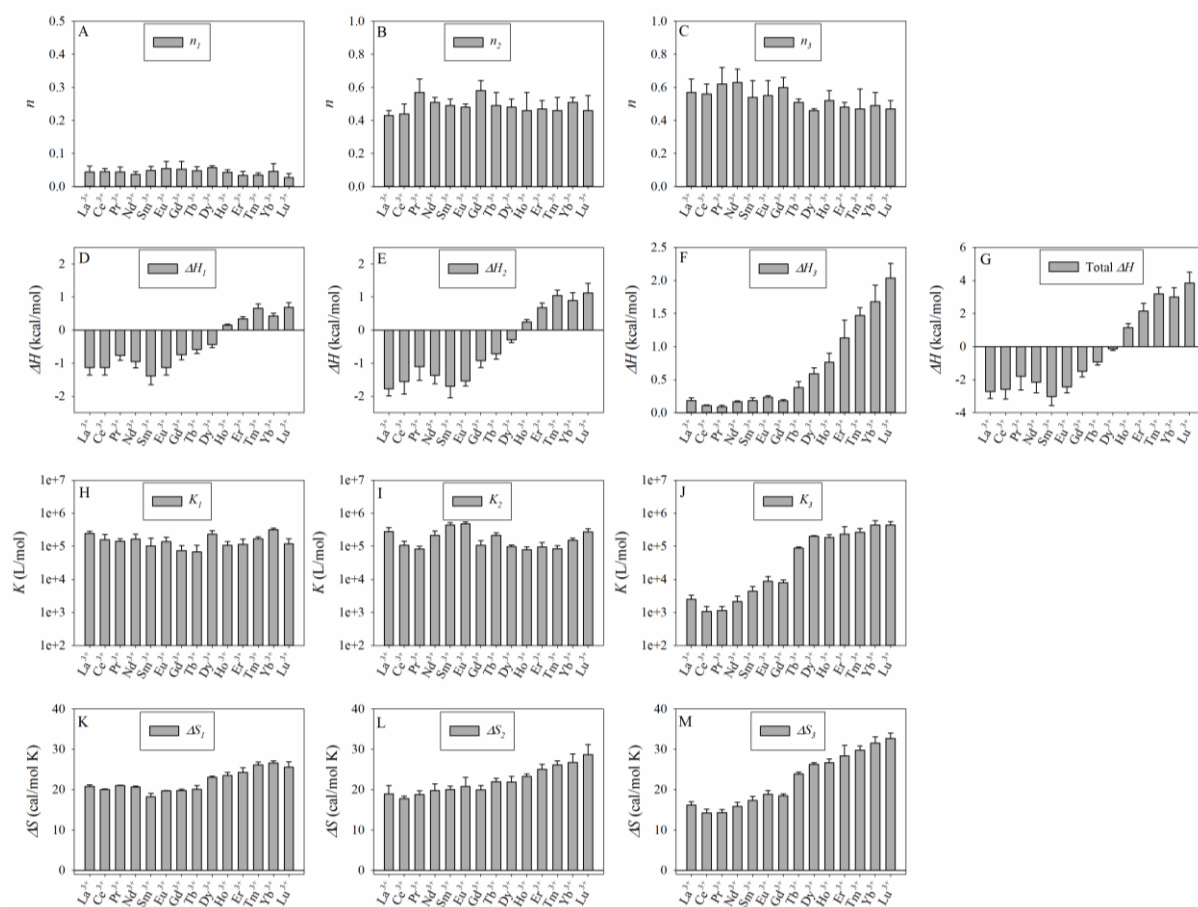


**Fig. 3.** The thermodynamic trends of Ln<sup>3+</sup> titrated into GMP solution based on a three-site model: (A-C) the binding ratio,  $n$ , between Ln<sup>3+</sup> and GMP; (D-G) reaction enthalpy; (H-J) binding constant; (K-M) reaction entropy. The total enthalpy change for all the three sites added together is presented in (G).

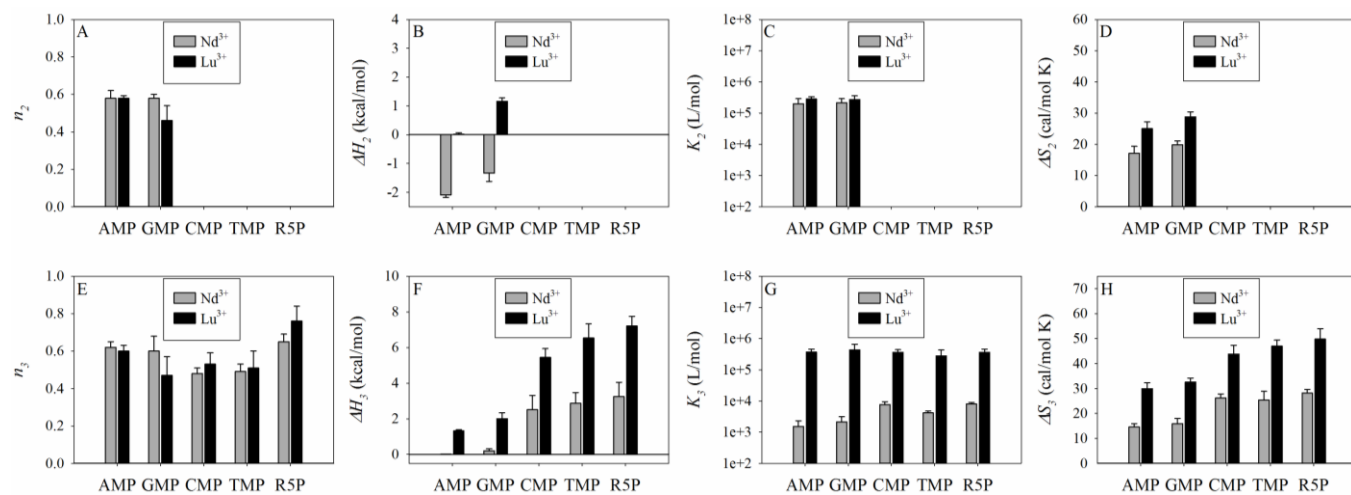


**Fig. 4.** Comparison of different nucleotides and R5P for binding  $\text{Nd}^{3+}$  and  $\text{Lu}^{3+}$  ions in terms of binding stoichiometry (A, E), enthalpy (B, F), binding constants (C, G) and entropy (D, H) for binding site 2 (A-D) and 3 (E-H). Data for site 1 are not plotted due to the very small binding ratio.

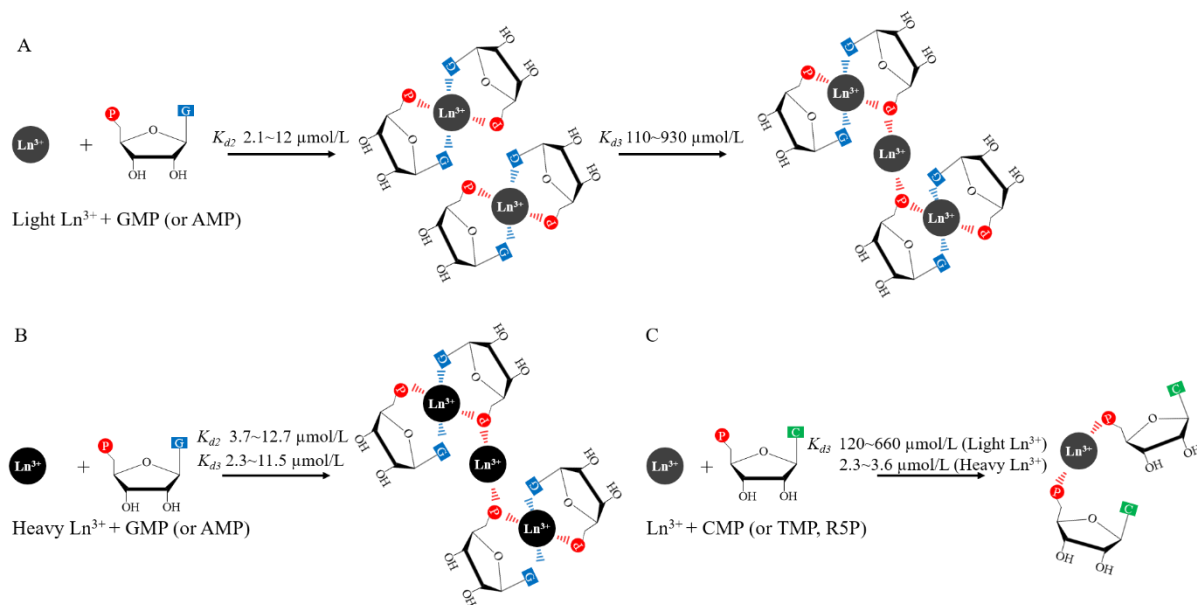


**Fig. 5.** A scheme showing the coordination interactions. (A) For GMP and AMP interacting with light  $\text{Ln}^{3+}$  (La to Gd), the phosphate and the base first chelate  $\text{Ln}^{3+}$ . With further additions of  $\text{Ln}^{3+}$ , the remaining coordination power of the phosphate is used. (B) For GMP and AMP interacting with heavy  $\text{Ln}^{3+}$  (Tb to Lu), the phosphate and the base bind nearly simultaneously ( $K_2$  and  $K_3$  ranges are nearly equal). Drawing is a simplified cartoon and does not represent the exact coordination number. For example, initially more than two GMP should be coordinated to each  $\text{Ln}^{3+}$  at low  $\text{Ln}^{3+}$  concentrations. (C) For CMP and TMP, the phosphate part is playing the main coordination role with little base involvement, similar to that of R5P.